The Complete Modeling Of The Image Formation In X-ray Lithography

Srinivas B. Bollepalli, M. Khan and F. Cerrina

Department Of Electrical & Computer Engineering
University of Wisconsin-Madison
Madison, WI 53715
sbollep@xraylith.wisc.edu, khan@xraylith.wisc.edu, cerrina@xraylith.wisc.edu

ABSTRACT

In the fabrication of semiconductor devices using lithography, the modeling of the exposure process is very often needed. The elements of a typical exposure system from a modeling perspective comprise of a radiation source, a patterned mask and a wafer coated with a photo-resist. The diffracted image of the mask pattern exposes the photo-resist after propagating through a distance termed *mask-to-wafer gap*. The exposed wafer is later on chemically developed to form a semiconductor device. In short, the electric field propagates through a series of regions (*layers*) with various materials and topographies (*structures*) before forming an image on the wafer.

In this paper we describe a computational algorithm based on *angular spectrum propagation* approach to model image formation in layered structures with particular emphasis to X-ray Lithography (XRL). Several illustrative examples will be presented.

Introduction

The modeling of X-ray Lithography (XRL) image formation [1,2] is based on the Fresnel approximation of the diffracted electric field. The complication of image formation in XRL stems from the system itself: mask topography, absorber side-wall slope variations, non-uniformities, materials, roughness in the mask and so on. To solve all these problems, a simulator, *CXrl Toolset*, based on a "layering" approach was created. In this method, the whole system - mask, gap, resist, wafer - is modeled as a sequence of non-uniform layers. With this, arbitrary mask and resist structures can be modeled as long as the in-plane distribution of the materials is known. The mask presents the most challenging problem - topography. In order to simulate this, an "ideal" mask pattern is subjected to a sequence of transformations. Some of these transformations include rounding of corners of a polygon, expansion or shrinking of features etc. This structure is then modeled as a series of thin transmission layers used in image calculations. The image is propagated from layer to layer by using classical scattering approach. A typical layered system is shown in above figure. In the application of modeling to harder X-rays (like those used in LIGA) it is necessary to take into account other effects. In particular, X-ray fluorescence must be included. The modeling approach and algorithm will be discussed in detail in the paper. An excellent agreement has been obtained with other detailed approaches. Several applications, such as modeling defects in masks, focusing of Fresnel zone plates etc. will be shown to illustrate the modeling for both MEMS and ULSI problems.

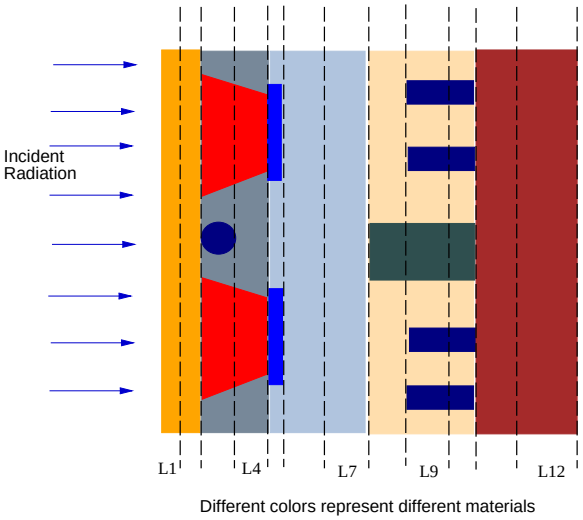

Figure 1: Illustration of layered system

The organization of the paper is as follows. First we introduce the well known concept of *angular spectrum of plane waves* which is used to describe diffraction in layered media. A sequential description of the propagation of fields from the mask plane to the wafer plane is given including the photo-absorption of energy by the resist. Then, the computational modeling of the resist dissolution is presented in detail. Finally, the modeling methodology is illustrated through several case studies done using the *CXrL toolset*.

Diffraction in layered media

Angular Spectrum of Plane Waves

Let a monochromatic wave field $E(x, y, 0)$ produced by a collection of monochromatic waves be incident on the $z = 0$ plane. The Fourier transform of $E(x, y, 0)$ can be written as

$$FE_0(f_x, f_y) = \int\int_{-\infty}^{\infty} E(x, y, 0) e^{-j2\pi(f_x x + f_y y)} dx dy \qquad (1)$$

$E(x, y, 0)$ can be represented in terms of its Fourier transform as

$$E(x, y, 0) = \int \int_{-\infty}^{\infty} FE_0(f_x, f_y) e^{j2\pi(f_x x + f_y y)} d f_x d f_y \quad (2)$$

The exponential part under the integral, can be regarded as an unit amplitude plane wave propagating in the direction

$$\hat{k} = (\lambda f_x)\hat{x} + (\lambda f_y)\hat{y} + \sqrt{1 - (\lambda f_x)^2 - (\lambda f_y)^2}\hat{z} \quad (3)$$

This decomposition of $E(x, y, 0)$ into plane waves propagating in various directions, with complex amplitudes $FE_0(f_x, f_y)$ is known as *angular spectrum* representation.

Propagation of the angular spectrum

Given $E(x, y, 0)$ we are interested in obtaining the field at a distance z, i.e., $E(x, y, z)$. Since $E(x, y, z)$ is assumed to be a scalar wave field, it must satisfy Helmholtz's equation at all source-free points,

$$\nabla^2 E + k_z^2 E = 0 \quad (4)$$

Substituting $E(x, y, z)$ by its angular spectrum representation and solving the above wave equation, it can be shown that

$$FE_z(f_x, f_y) = FE_0(f_x, f_y) exp[j(\frac{2\pi}{\lambda})\sqrt{(1 - (\lambda f_x)^2 - (\lambda f_y)^2}z] \quad (5)$$

where $FE_0(f_x, f_y)$ is the Fourier transform of the incident field $E(x, y, 0)$. Therefore, we can write

$$E(x, y, z) = \int \int_{-\infty}^{\infty} FE_0(f_x, f_y) exp[j(\frac{2\pi}{\lambda})\sqrt{(1 - (\lambda f_x)^2 - (\lambda f_y)^2}z] \quad (6)$$

which describes the propagation of the angular spectrum. The validity of *angular spectrum* propagation has been studied by several authors and conditions for validity have been given in [3,4].

Transmission function of a layer

Consider a planar inhomogeneous layer of thickness d extending from $z = 0$ to $z = d$. At X-ray wavelengths (1 nm), the refractive indices of any material is complex, with real part being close to unity and a very small imaginary part as shown below.

$$\tilde{n} = n + j\kappa \quad (7)$$

Thus the effect of the propagation through a space z filled with uniform material can be written:

$$exp[j\, kz] = exp[-\kappa\, k_0 z] exp[j\, nk_0 z] \quad (8)$$

The first exponential represents the attenuation due to the propagation through a distance z, and the second the corresponding phase shift. Notice that $n = Re(\tilde{n})$ appears explicitly in the exponential, effectively increasing the optical thickness of the medium to $n\ z$. Finally, Eq. 8 represents the transmission function, which is position dependent and yields:

$$t(x, y) = exp[-\kappa(x, y)\, k_0 z] exp[j\, n(x, y) k_0 z] \quad (9)$$

In this equation, both κ and n are position dependent, and can be supplied in a bitmap form where each pixel has a transmission given by Eq. 13. Notice further that all the optical properties *of the layer* have been collapsed into the transmission function.

Propagation through a layer

Thus the propagation of a scalar wave field through a layer can be obtained in two steps.

- By multiplication of the incoming wave-field with the transmission function of the layer
- Propagating the angular spectrum of the modulated wave field through a distance equal to the thickness of the layer.

They are described below. *Assuming that the thickness of the object is negligible,* the field *right after* the object will be:

$$E_t(x, y) = E_{in}(x, y) t(x, y) \quad (10)$$

where E_{in} represents the incoming plane wave. Here, we are implicitly applying Kirchoff boundary conditions and assuming that the incoming wave field is not disturbed and that it is only modulated. For sufficiently thin layers, this is a good approximation [5,6].

In general, we can write the transmission of the layer using its Fourier representation:

$$t(x, y) = \int d\nu_x d\nu_y T(\nu_x, \nu_y) exp[-j2\pi(x\nu_x + y\nu_y)] \quad (11)$$

This is equivalent to decomposing the transmission object in a sum of infinite diffraction gratings, specified by the frequencies (ν_x, ν_y). Each will contribute to scatter the plane wave, with a weight proportional to the component T of the transmission function at that frequency.

After the wave has been transmitted through the layer, it will propagate through free-space until it reaches the image plane, located at a distance z. Essentially nothing will happen to the plane waves as they propagate; after moving a distance z, the wave is described by Eq. 15. Thus, the central idea is that *a plane wave is modulated by an object of transmission function $T(x, y)$, filtered into a new set of plane waves which are then propagated through free space.* As stated, this represents the *Fresnel-Kirchoff Approximation* of the diffraction theory. In a layered media as shown in figure 1, the field is propagated layer by layer. The diffracted field from the *i*th layer is the incident field for *(i+1)*th layer, from which the computational scheme can be easily obtained.

Dose absorption in resist

The absorbed dose in the resist is defined as the amount of energy absorbed per unit volume. Given a resist of thickness Z_r, the change in intensity inside the resist between depths, z and $z + dz$ as a function of depth z can be written as

$$dI(z, \omega) = I(z, \omega)\alpha(\omega) dz \quad (12)$$

where $\alpha(\omega)$ is the absorption coefficient and $I(z,\omega)$ is magnitude squared of the wave field at Z. $I(z,\omega)$ can be expressed as a function of the incoming intensity at the surface of the resist as

$$I(z) = \int I(0,\omega)e^{-\alpha(\omega)z}d\omega \tag{13}$$

When integrated over time we get the delivered dose (mJ/cm^3).

Mathematical modeling of resist dissolution

To model the resist dissolution process, we first separate the model space into two disjoint sets to create the "initial front": resist and developer; once the two regions are formed, and then the dissolution model tracks the "developer-resist interface" as a function of time, where the speed of the front propagation at each grid point is a function of the *dose*, *depth* and *envelope feature size* at that grid point. We then employ the *Fast Marching Level Set* technique, developed by Sethian [7], to track the interface. In this paper, we provide just an overview of the numerical technique; for detailed discussion of this technique, see [7].

Equations of Motion of the Front

Consider a boundary, separating one region from another, which moves in normal direction with speed $F = F(x,y,z)$. Also suppose we know that the boundary is a monotonically advancing front such at $F > 0$ (eg., the precondition that resist can never be "undeveloped"). Sethian [7] shows that this advancement problem can then be transformed into a **stationary** problem where time is no longer an independent variable. In essence, instead of solving for the front position at each time step, we solve, at each grid point, the time when the front *crossed* that point.

Following the discussion in [7], let $T(x,y,z)$ be the time at which the boundary crosses the grid point (x,y,z). The boundary $T(x,y,z)$ then satisfies the equation:

$$|\nabla T(x,y,z)|R(x,y,z) = 1 \tag{14}$$

This is the well known *Eikonal equation* from geometrical optics. The position of the front, Γ at a time t is given by the level set (contour) of value t of the function $T(x,y,z)$, that is

$$\Gamma(t) = \{(x,y,z)|T(x,y,z) = t\} \tag{15}$$

To find the front at time t, simply take the level set (contour) of the function at time t. To solve

$$|\nabla T(x,y,z)| = \frac{1}{R(x,y,z)} \tag{16}$$

we use a finite difference scheme with the following gradient operator (for an one-dimensional case):

$$|T_x| \approx [(max(D_i^{+x}T,0)^2 + min(D_i^{-x}T,0)^2)]^{1/2} \tag{17}$$

where we use the standard finite difference notation for 1-dimensional T_x:

$$\begin{aligned} D_i^{0x}T &= \frac{T_{i+1} - Ti - 1}{2h} \\ D_i^{-x}T &= \frac{T_i - Ti - 1}{h} \\ D_i^{+x}T &= \frac{T_{i+1} - Ti}{h} \end{aligned}$$

T_i is the value of T at point ih with grid spacing h.

Once we obtain the parameters needed to solve Equations 16 and 17, we follow the "Narrow Band" algorithm outlined by Sethian [7] to solve for $T(x,y,z)$ on a Cartesian grid. Once we compute $T(x,y,z)$, we can then animate the dissolution process by simply "contouring" the volume at specific time-steps.

Implementation

The exposure system is modeled using solid geometry techniques and by slicing this system we get a layered description. The numerical code for the diffraction calculations as well as the resist dissolution is written in C++ and integrated in EXCON [8] to enable complex simulation studies; the GUI is written in a combination of C++, Tcl and Tk, and uses The Visualization Toolkit for 3D rendering.

Illustrative Examples

The patterning ability of X-ray lithography is best illustrated by considering the propagation of the diffracted image through the gap. In figure 2, a truncated grating with minimum feature size of 0.25μm is considered and the diffracted image at various gaps is shown. Figure 3 shows the propagation of 2-dimensional fields in a layered system. Notice the increase in contrast of the aerial images due to absorption in the layers.

Defects in X-ray masks are caused by errors during mask fabrication and by contamination while using the mask for printing [9]. The effect of defects in the X-ray mask can be easily simulated with the layered approach. An example of a stainless steel defect present between two lines of an absorber pattern is shown in figure 4. The developed resist (APEX-E) is shown in figure 5.

It is well known that point sources provide an alternate to synchrotron radiation for X-ray lithography. Point sources are characterized by a source divergence angle θ_s and a global divergence angle θ_g. As a result, the fields at the corners and edges of the mask receive an oblique illumination if a collimator is not used. The result of developing a complex mask pattern to such an oblique illumination (20 mrads) is shown in figures 6 and 7. Notice that the resist side-walls are slanted.

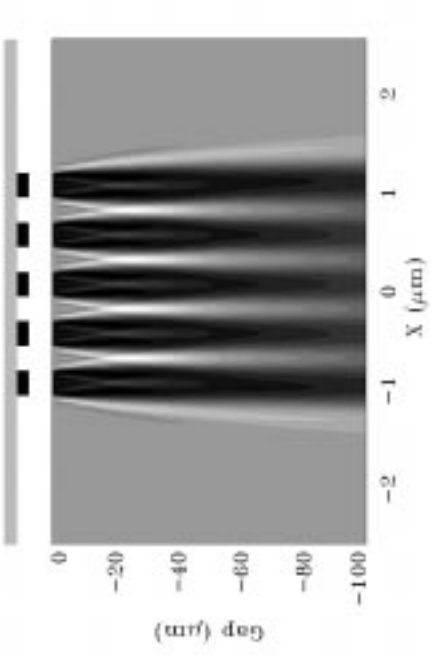

Figure 2: Diffraction of X-rays

Extension to EUV Lithography

The modeling techniques described in this paper can be easily adapted to the case of EUV lithography where a reflective mask is used. The computations are more intensive along with the added feature that, at each interface we have reflected fields. The details of computation of reflected images from reflective multilayer masks is presented in [10]. Figure 7(a) shows the propagation of fields within the EUV mask for oblique incidence (10 degrees). Figure 7(b) shows the reflected image of a square pattern (CD = 400nm). Notice the asymmetry of edges due to oblique incidence.

Conclusions

In this paper we have described the modeling of image formation in layered structures using the angular spectrum propagation approach. Several examples have been presented as application to X-ray lithography. The use of the angular spectrum approach is computationally very efficient, as the the image propagation is carried out using Fourier transforms from layer to layer. However, for very large grid sizes, this may cause requirements for large memory. We have implemented a new resist dissolution model that is numerically stable under arbitrarily complex geometries and shows extendibility across multiple lithographic technologies and across application domains from very small features used in DRAMs ($\leq 70nm$) to very large patterns ($\geq 10\mu$) used in MEMS devices. It is however necessary to have good characterization of the resist dissolution process to be able to accurately predict the final profile. Future work will focus on better characterization of chemically amplified resist dissolution process, and to parameterize the dissolution rate as a function of depth and feature size in addition to the absorbed dose.

REFERENCES

[1] B.E.A. Saleh and M.C. Teich, *Photonics*, p.111-121, Wiley 1991

[2] J.W. Goodman, *Introduction to Fourier Optics*, McGraw-Hill, 1968

[3] W.H. Southwell, *Validity of the Fresnel Approximation in the near field*, JOSA, **71**, 7-14 (1981), Eqs. 7-9.

[4] E. Lalor, *Conditions for the Validity of the Angular Spectrum of Plane Waves*, JOSA, **58**, 1235 (1968)

[5] Cerrina F., *X-ray Lithography*, Chapter 3, Handbook of Micro-lithography, Micro-machining and Micro-Fabrication, Volume 1, 1997.

[6] Guo Z. Y., Cerrina F., *Modeling Proximity Lithography* ,IBM Journ. Res. Develop., **37** 331, (1993).

[7] J. A. Sethian, "Level Set Methods", Cambridge University Press, 1996.

[8] M. Khan, P. D. Anderson, and F. Cerrina, Proc. SPIE, **1465**, 315 (1991).

[9] B. S. Bollepalli, S. D. Hector, J. Maldonado ,J. A. Leavey , F. Cerrina, M. Khan, *Simulation of X-ray mask defect printability*, Proc. SPIE, Vol 3048, pp 155-166, Emerging Lithographic Technolgies;David E. Seeger, Ed;

[10] B.S.Bollepalli, M.Khan, F.Cerrina, *Imaging properties of EUV masks*, to be published in J. Vac. Sci. Technol., Nov/Dec issue, 1998.

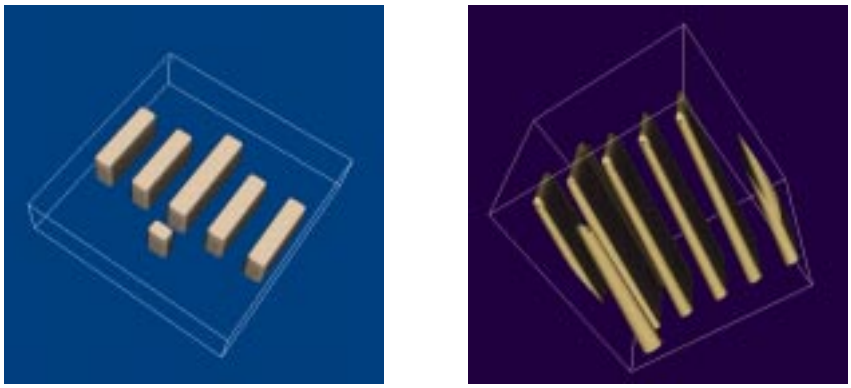

(a) Mask pattern (b) Developed resist profile

Figure 3: Simulation of resist exposed by point source

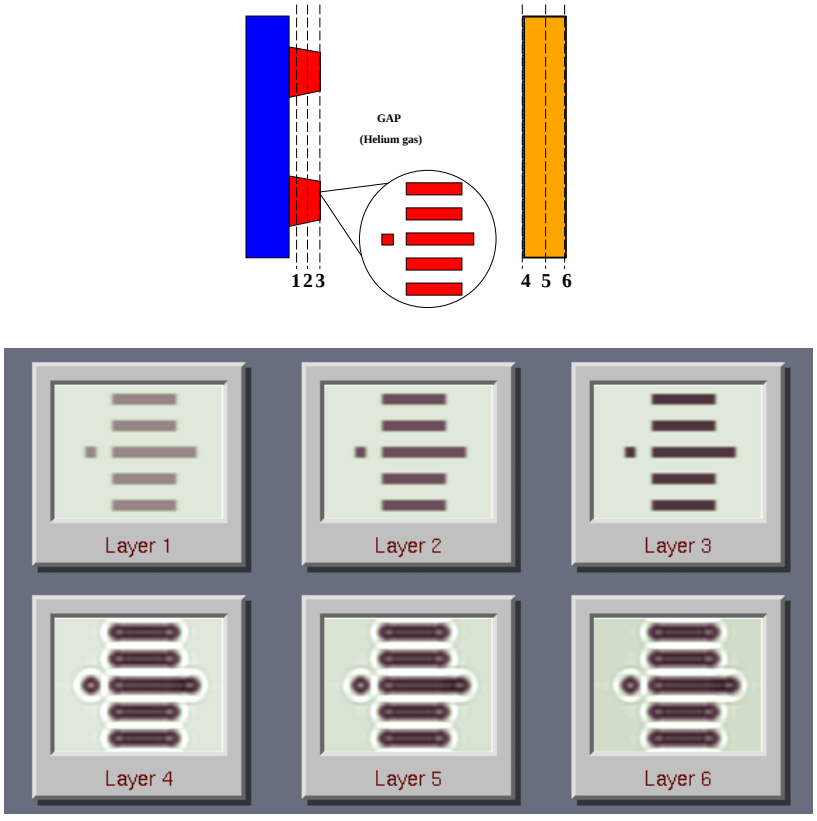

Figure 4: Image propagation from layer to layer

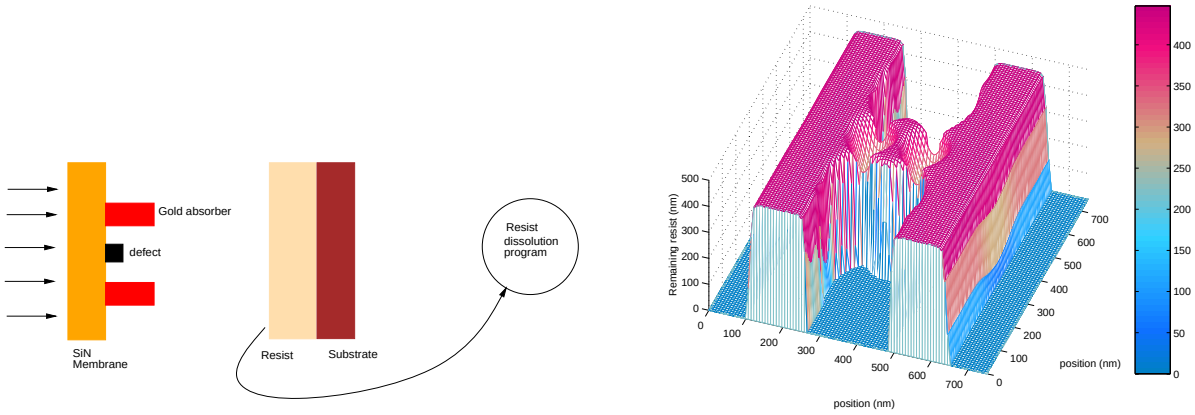

(a) Mask Pattern

(b) resist profile

Figure 5: Effect of a mask defect on developed resist

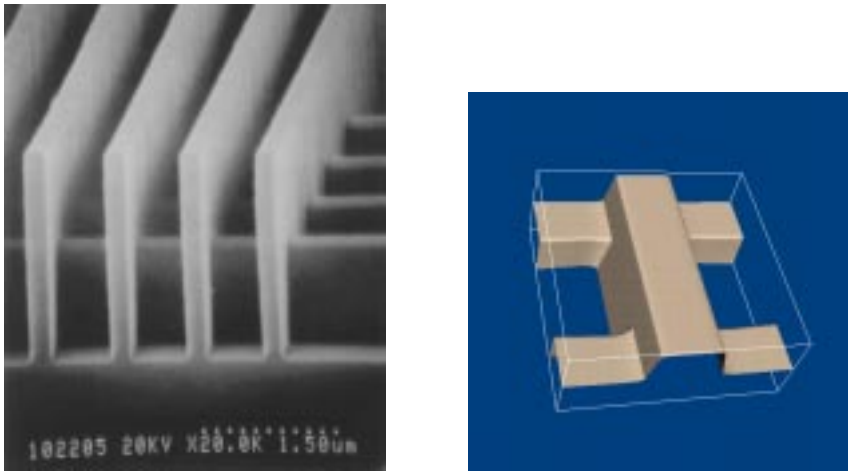

(a) SEM micrograph (K. Deguchi, NTT)

(b) Developed profile

Figure 6: Resist dissolution over pre-existing topography I

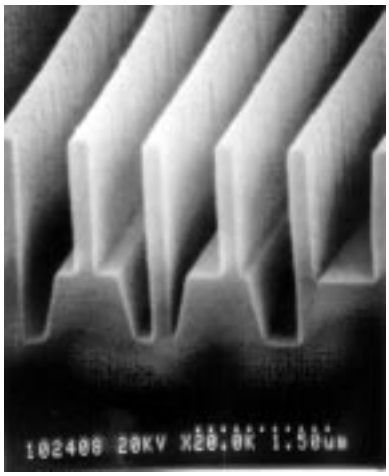

(a) SEM micrograph (K. Deguchi, NTT)

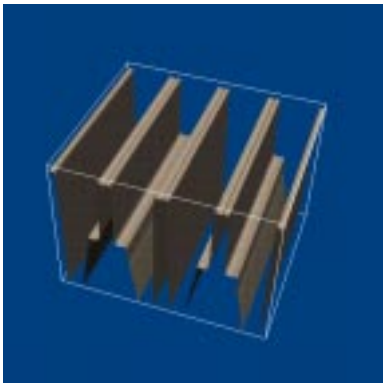

(b) Developed profile

Figure 7: Resist dissolution over pre-existing topography II

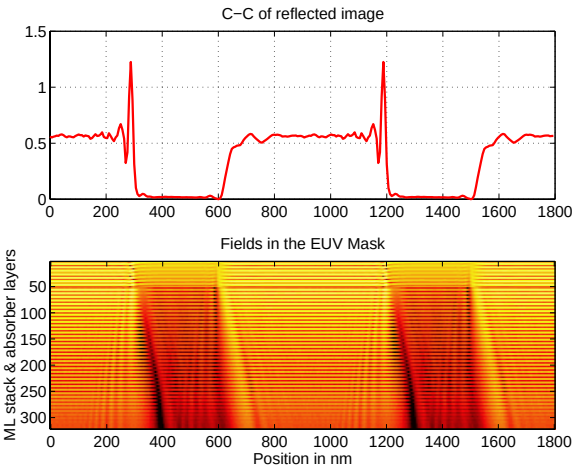

(a) Propagation of field in the EUV mask

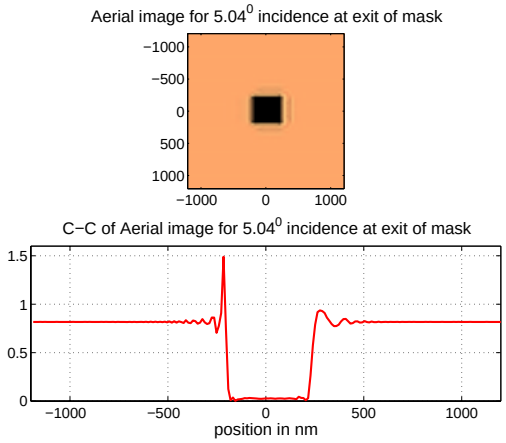

(b) Reflected image of a square pattern (CD = 400nm)

Figure 8: Extendibility of the toolset to EUV lithography